



Research article

Study on the effect of multi-source solid waste on the performance of its backfill slurry

Xinyuan Zhao^{a,c}, Ke Yang^{b,c,*}, Zhen Wei^{a,c}, Xiang He^{a,c}, Ruiyi Chen^{a,c}^a State Key Laboratory of Mining Response and Disaster Prevention and Control in Deep Coal Mine, Anhui University of Science and Technology, Huainan, 232001, China^b Institute of Energy, Hefei Comprehensive National Science Center, Hefei, 230000, China^c School of Mining Engineering, Anhui University of Science and Technology, Huainan, 232001, China

ARTICLE INFO

Keywords:

Multi-source solid waste
Underground backfilling
Backfill slurry
Thermal stability
Mechanical property
Coal-based solid waste

ABSTRACT

The preparation of slurry from multi-source solid waste for underground backfill adds a way out for solid waste disposal, which is beneficial to reduce environmental impact. In this paper, the effects of gangue, fly ash, gasification coarse slag and desulfurization gypsum on the fluidity, early strength, thermal stability and other properties of the backfill slurry were studied by fluidity test, strength test, Thermo-Gravimetric Analysis (TGA), Scanning Electron Microscope (SEM) and X-ray Diffraction (XRD). The results show that: (1) When G/SW (mass ratio of gangue to solid waste) < 23%, gangue is beneficial to improve the fluidity and early strength of backfill slurry; with the increase of fly ash content, the fluidity of backfill slurry decreases, but its early strength increases; gasification coarse slag has a negative effect on the fluidity of backfill slurry, but it is beneficial to its early strength when GCS/SW (mass ratio of gasification coarse slag to solid waste) < 33%; desulfurization gypsum can improve the fluidity of the backfill slurry, but it is not conducive to the increase of early strength. (2) The compression failure mode of the backfill is mainly divided into the crack-intensive failure, the single main crack penetration splitting failure, and the double main crack conjugate splitting failure. (3) Endothermic dehydration reactions of adsorbed water and crystallization water generally occur at 55–65 °C and 110–130 °C for backfill with different solid waste contents; As the temperature continues to increase, the backfill material undergoes a slow exothermic decomposition reaction; Increasing the content of gangue, fly ash and gasification coarse slag and reducing the content of desulfurized gypsum can make the backfill less weight loss at high temperature and better thermal stability. (4) The main mineral phases in the backfill material are gypsum and quartz, and there are also a small amount of acicular and hexagonal hydration products thaumasite. After high temperature, the thaumasite is dehydrated and decomposed. The research results are helpful to deeply understand the performance of multi-source solid waste for underground backfilling.

1. Introduction

Many coal mines, power plants and coal chemical plants are distributed in Western China. A large number of industrial solid wastes are produced in this area every year, such as coal gangue, fly ash, gasification coarse slag and desulfurization gypsum, resulting in

* Corresponding author. Institute of Energy, Hefei Comprehensive National Science Center, Hefei, 230000, China.

E-mail addresses: xinyuan.zhao@unito.it, 386308458@qq.com (X. Zhao), keyang@aust.edu.cn, keyang2003@126.com (K. Yang).<https://doi.org/10.1016/j.heliyon.2023.e16251>

Received 11 September 2022; Received in revised form 5 May 2023; Accepted 10 May 2023

Available online 16 May 2023

2405-8440/© 2023 Published by Elsevier Ltd. This is an open access article under the CC BY-NC-ND license (<http://creativecommons.org/licenses/by-nc-nd/4.0/>).

adverse environmental problems including water, soil and air pollution [1,2]. The large-scale disposal and utilization of solid waste have become a difficult problem for local companies and governments [3]. Some local coal mines try to backfill the underground space with solid waste that meets environmental protection standards in the form of slurry, to achieve the effect of controlling multiple hazards [4–6], as shown in Fig. 1.

The key to realizing large-scale underground backfilling of solid waste slurry is the fluidity and early strength of the backfill material. The fluidity affects the transportation and backfilling efficiency of the backfill slurry, while early strength affects the rock stratum control effect after backfilling [7–10]. Many scholars have done a lot of research work on the physical and mechanical properties of mine backfilling materials. Fall et al. [11] took the uniaxial compressive strength, slump and solid concentration of cemented tails backfill as indicators, and proposed the mixture design method and performance prediction model of cemented tailings backfill; Zhang et al. [12] obtained the optimal mix ratio of coal-based solid waste cemented filling through orthogonal experiments, and studied its mechanical properties and fluidity; Wei et al. [13] studied the effects of slurry concentration, binder content and fly ash addition on the flow characteristics of backfill materials; Chen et al. [14] optimized the fluidity and strength of gasified slag-based paste backfill materials by using the central composite experiment method, and analyzed the microscopic morphology; Koohestani et al. [15] compared and studied the effects of different admixtures on the flow behavior, strength development and microstructure characteristics of cemented paste backfill composed of sulfide and non-sulfide. Tang et al. [16] studied the mechanical properties and effects of each component before and after the mix proportion optimization of backfill material from coal-based solid waste; Cavusoglu et al. [17] studied the effect of sodium silicate as an accelerator on the early mechanical and microstructure properties of cemented coal fly ash backfill; Zhao et al. [18] explored the influence of loess content on the fluidity and mechanical properties of paste backfill materials; Jiang et al. [19] studied the effects of aggregate gradation, sand addition and binder content on the uniaxial compressive strength and stress-strain characteristics of cemented rockfill. There are also literature studies on the effects of fly ash and gangue on the fluidity and early strength of the slurry. For example, fly ash has a certain lubricating effect on cement paste due to its ball effect, but the water absorption effect of fly ash will also reduce the fluidity of cement paste in the later stage [20]; Due to its secondary hydration, fly ash is beneficial for the later strength improvement of the paste, but due to the hindering effect of the thin layer of vitreous body on the surface of fly ash particles, the 1-day strength of the material is decreased [21]. The literature has studied the influence of gangue particle size and gradation on the fluidity and strength of materials, and shows that high content of gangue with large particle size is not conducive to the increase of fluidity and later strength of materials [22]. The related research results of different types of mine solid waste backfill materials are abundant [23–28]. A new slurry material suitable for pipeline pumping and for grouting and backfilling in underground goaf is prepared by mixing the multi-source solid wastes, such as gangue, fly ash, gasification coarse slag and desulfurization gypsum. At present, the research and application of this solid waste backfill material are still in their infancy. There are still many properties and mechanisms of this backfill material that are still unclear, such as the effect of various solid waste components on its fluidity, early strength and micro characteristics, so it is necessary to conduct research on relevant content before this multi-source solid waste is backfilled underground.

In this paper, the effects of gangue, fly ash, gasification coarse slag and desulfurization gypsum on the properties of solid waste backfill slurry were studied by fluidity test, strength test, TGA, SEM and XRD. This study is helpful to understand the feasibility of multi-source industrial solid waste for underground backfilling, and provides a basis for the ratio optimization of backfill materials from multi-source solid waste.

2. Experimental materials

2.1. Physical characteristics

The four solid wastes in this experiment are gangue, fly ash, gasification coarse slag and desulfurization gypsum, all of which are

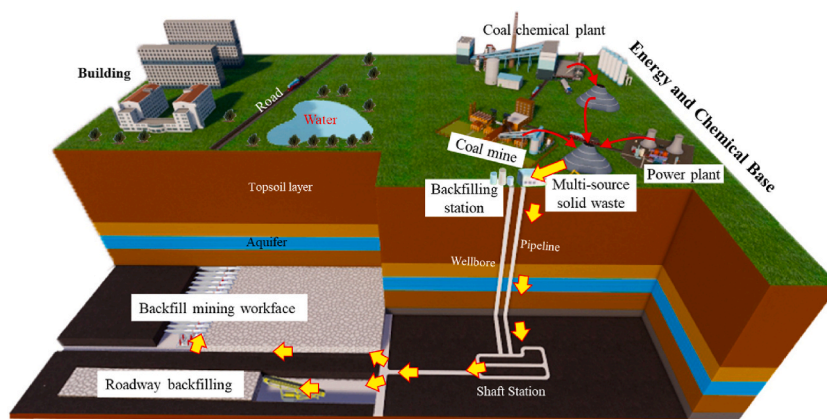


Fig. 1. Schematic diagram of multi-source solid waste for underground backfilling.

Class I industrial solid waste from Ningdong Base in China, adding a small amount of cement as a cementitious material. The experimental materials are shown in Fig. 2.

(1) Gangue

The coal gangue comes from a coal mine in Ningxia, China. The lithology is mainly sandstone and shale. It is hard and gray-black, as shown in Fig. 2(a). The original gangue has a large grain size and needs to be broken and screened. The gangue with a grain size less than 15 mm is as the experimental material. Three bags of samples (about 2 L per bag) are randomly taken in the mixed uniform gangue material, and then screened and weighed. Calculate the percentage of sample mass in each particle size range to the total mass and take the average value, as shown in Table 1. It can be seen that the mass proportion of gangue with a particle size range of 5.00–10.00 mm is the largest, followed by 10.00–15.00 mm and 2.50–5.00 mm, and the particle size range with the smallest mass proportion of gangue is 1.25–2.50 mm.

(2) Fly ash

The fly ash (Fig. 2(b)) in the experiment is second-class powered coal ash, with a fineness of 20, a loss on ignition of 2.50%, a specific surface area of 481.20 m²/kg, the water content of <1.00%, off-white, powdery. The particle size distribution results of fly ash are shown in Fig. 3. It can be seen that the grain size range of fly ash in this experiment is basically 0.30–300 μm, with about 100 μm accounting for the largest proportion, and less than 100 μm accounting for about 85% of the total volume.

(3) Gasification coarse slag

The gasification coarse slag (Fig. 2(c)) is black, granular, with a specific surface area of 1469 m²/kg and a water content of about 10%. It can be seen from Fig. 3 that the grain size distribution curve of gasification coarse slag presents a bimodal shape, the grain size range is basically 0.20–300 μm, the proportion with the grain size range of about 140–160 μm is the largest, followed by about 6–8 μm, and the grain size below 150 μm accounts for about 90%.

(4) Desulfurization gypsum

Desulfurization gypsum (as shown in Fig. 2(d)) is dark yellow, with a specific surface area of 367.10 m²/kg and a water content of about 5%. It is blocky and can be broken into powder after drying, with a certain sense of lubrication. The grain size distribution range of desulfurization gypsum is basically 0.50–400 μm, the grain size of about 30 μm accounts for the largest percentage, and the grain size of less than 30 μm accounts for more than 70%.

(5) Cement

The cement comes from a mine in Ningxia, as shown in Fig. 2(e), with the cement label PO32.5, gray-white, powdery, with a specific surface area of 652.10 m²/kg, and the volume with a particle size of less than 60 μm accounts for more than 90%.



Fig. 2. Experimental materials, (a)Gangue, (b)Fly ash, (c) Gasification coarse slag, (d) Desulfurization gypsum, (e) Cement.

Table 1
Percentage of gangue grain size.

Grain size interval	≤1.25 mm	1.25–2.50 mm	2.50–5.00 mm	5.00–10.00 mm	10.00–15.00 mm
Average percentage	14.00%	4.95%	16.95%	41.00%	23.10%

Note: The grain size interval includes only the upper limit.

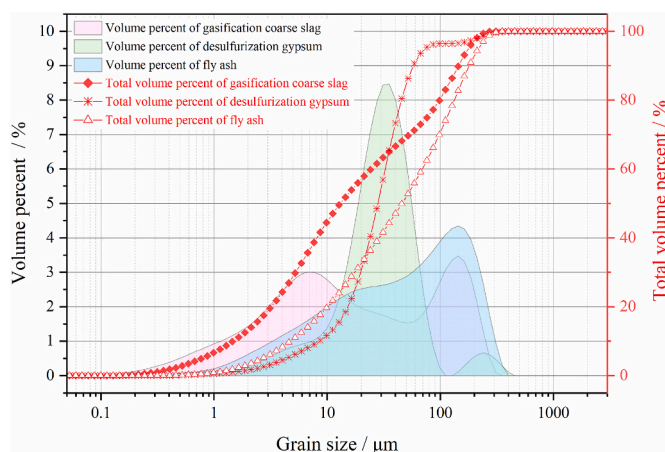


Fig. 3. Grain size distribution of three solid waste.

2.2. Component analysis

The mineral composition of the experimental materials is analyzed by XRD, as shown in Fig. 4. The chemical composition of the experimental materials measured by XRF is shown in Table 2.

The main mineral components of gangue are quartz and kaolinite. The main mineral components of fly ash are quartz and aluminium silicate, the main mineral component of desulfurization gypsum is gypsum, the main component of gasification coarse slag is quartz, and the main component of cement is gypsum and tricalcium silicate. In addition, gangue and fly ash contain traces of iron oxide and magnesium oxide, and cement contains traces of calcium carbonate.

Among the oxide components contained in gangue and desulfurized gypsum, CO₂ accounts for the largest proportion, indicating that these two materials have a large carbon content. The chemical composition of fly ash and gasification coarse slag is basically the same, and the oxides with higher content are SiO₂, CO₂, Al₂O₃, etc. The oxide with the highest content in cement materials is CaO, indicating that cement has a high calcium content.

3. Specimen preparation

3.1. Experimental scheme

The author's team conducted a proportioning experiment on gangue, fly ash and gasification slag in the early stage, and provided a proportioning experiment report to Ningxia Coal Industry Group and other enterprises. The report shows that the relatively optimal ratio with the comprehensive indexes (mainly fluidity and early strength) of the backfill slurry composed of gangue, fly ash and gasification coarse slag is FA: GCS: G = 3:4:1, and the mass concentration is 77%. The slump of the backfill slurry with the optimum ratio is 134 mm, the slump-flow is 383 mm, and the 1-day strength and 3-day strength are 0.23 MPa and 0.35 MPa, respectively. In this experiment, desulfurization gypsum is added on the basis of the above three solid waste materials, and the backfill slurry is composed of four solid waste materials. In order to reduce the workload and fully study the effect of gangue (G), fly ash (FA), gasification coarse slag (GCS) and desulfurization gypsum (DG) on the performance of backfill slurry, the single-factor transformation method was used to design the experimental scheme for the backfill slurry composed of four solid wastes. First, the initial mass proportion between the four solid waste materials is set as FA:GCS:DG:G = 3:4:3:1, and the mass concentration is taken as 76% and 78% respectively. Then one solid waste is selected as a variable factor in turn, its relative proportion is set as an integer from 1 to 5, the relative proportions of the other three solid wastes remain unchanged. The mass percentages of the corresponding variable factors in the total solid waste (SW) are calculated, such as FA/SW, GCS/SW, DG/SW and G/SW. To reduce the backfilling cost as much as possible, the cement content is set to 2% of the solid waste material consumption. The total amount of solid waste materials in each experimental group is set at 2 kg. The experimental scheme is shown in Table 3.

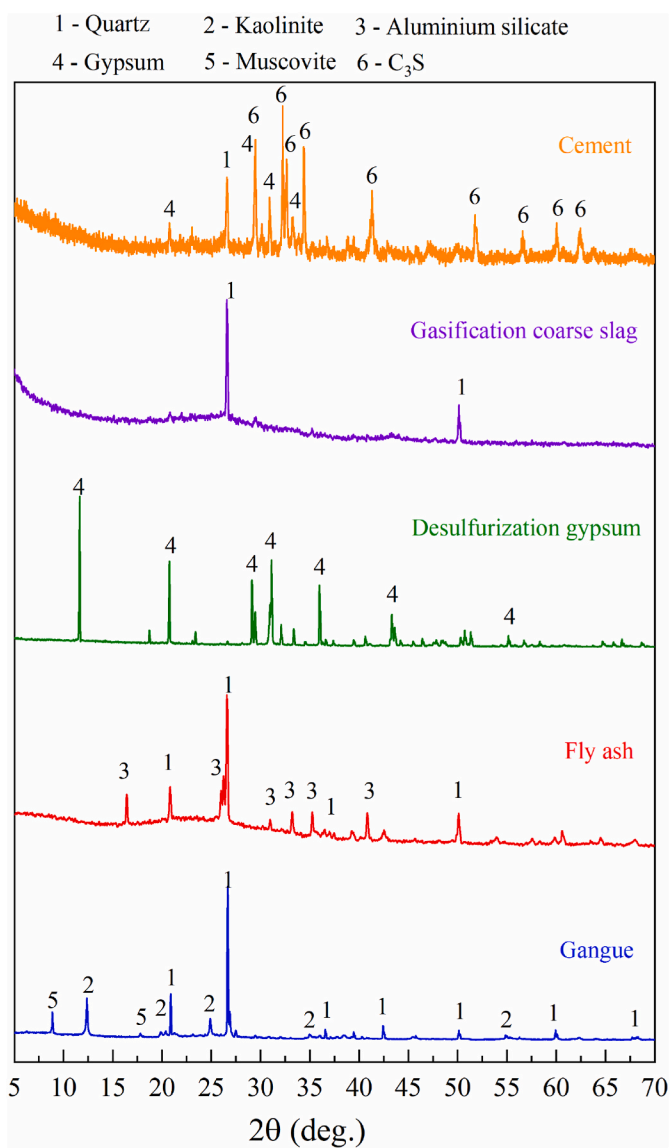


Fig. 4. XRD results of experimental materials.

Table 2

Test results of experimental materials.

Gangue/%		Fly ash/%		Desulfurization gypsum/%		Gasification coarse slag/%		Cement/%	
SiO ₂	13.16	SiO ₂	40.40	CO ₂	38.20	SiO ₂	38.80	SiO ₂	22.10
CO ₂	75.00	CO ₂	23.90	SO ₃	32.76	CO ₂	23.80	Al ₂ O ₃	5.62
Al ₂ O ₃	5.94	Al ₂ O ₃	19.00	CaO	23.36	Al ₂ O ₃	13.70	Fe ₂ O ₃	3.40
Fe ₂ O ₃	3.49	Fe ₂ O ₃	5.10	SiO ₂	2.26	CaO	8.52	CaO	65.54
K ₂ O	1.11	CaO	4.28	MgO	1.30	Fe ₂ O ₃	6.05	MgO	1.41
Others	1.30	Others	7.32	Others	2.12	Others	9.13	Others	1.93

3.2. Experimental method

(1) Preparation and curing of specimens

The operation methods of material weighing, mixing, specimen preparation and curing shall refer to the Chinese standard "Standard for Test Methods of Performance on Building Mortar" (JGJ/T70-2009). The material is weighed by mass. The material mixed

Table 3
Experimental scheme.

Variable factor	Mass concentration	FA: GCS: DG: G	Percentage of variable factors in solid waste
FA	76%, 78%	1: 4: 3: 1	11%
		2: 4: 3: 1	20%
		3: 4: 3: 1	27%
		4: 4: 3: 1	33%
		5: 4: 3: 1	39%
GCS	76%, 78%	3: 1: 3: 1	13%
		3: 2: 3: 1	22%
		3: 3: 3: 1	30%
		3: 4: 3: 1	37%
		3: 5: 3: 1	42%
DG	76%, 78%	3: 4: 1: 1	11%
		3: 4: 2: 1	20%
		3: 4: 3: 1	27%
		3: 4: 4: 1	33%
G	76%, 78%	3: 4: 5: 1	39%
		3: 4: 3: 1	9%
		3: 4: 3: 2	17%
		3: 4: 3: 3	23%
		3: 4: 3: 4	29%
3: 4: 3: 5	33%		

with water is mechanically stirred for 3 min. The evenly stirred material is poured into a mold with a length, width and height of 70.7 mm, and placed in a curing box. The curing conditions simulate the underground backfilling environment, with a temperature of 20 ± 2 °C and a humidity of $85 \pm 5\%$.

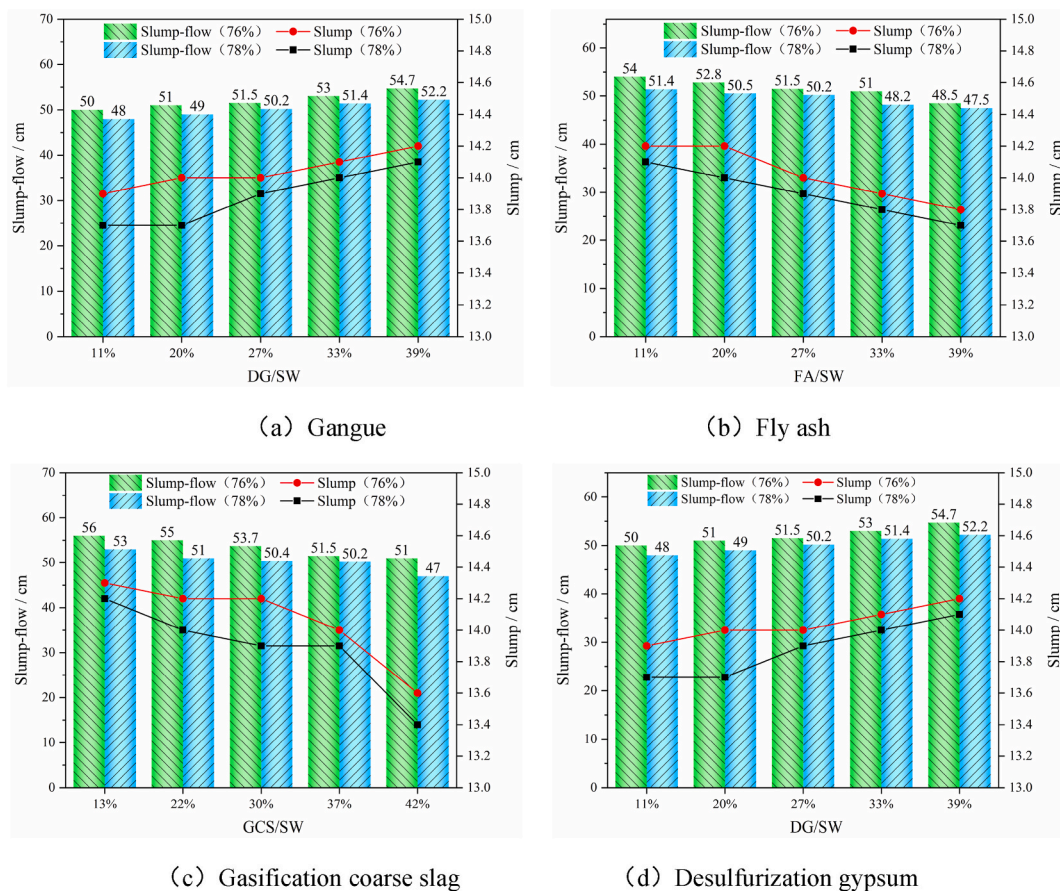


Fig. 5. Slump and slump-flow of backfill slurry.

(2) Liquidity test

The fluidity of the backfill material is characterized by slump, slump-flow and bleeding rate, that is, the bleeding rate is about 5%, and the greater the slump and slump-flow of the backfill material, the better its fluidity [29,30]. In this experiment, in order to save materials and preparation time, referring to the related literature [31,32], a small slump bucket was selected as the tool for measuring slump and expansion. The slump, slump-flow and bleeding rate of backfill material were carried out following the Chinese standard "Standard for Test Methods of Performance on Ordinary Fresh Concrete" (GB/T50080-2016).

(3) Early strength test

Since the specimen was not completely formed after curing for 1 day, the early strength of the specimen in this experiment is the compressive strength at the curing time of 3 days and 7 days. The length, width and height of the demoulded specimen are 70 ± 2 mm. Before testing, the surface of the specimens was ground flat. Due to the low strength of the test piece, the press adopts the stress loading method, the loading rate is 0.05 kN/s, and the failure load of the test piece is recorded.

(4) Microscopic test

To better evaluate the performance of the solid waste backfill, After the compression test of the backfill specimen, the micro-structure, phase and thermal stability of the backfill specimen were analyzed by SEM, XRD and TGA. The samples used in the TGA are backfill specimens with each variable factor relative proportions of 2 and 4, and curing times of 3-day and 7-day. The sample was heated to 800 °C in a dynamic N₂ atmosphere at a heating rate of 10 °C/min. In the XRD test, the continuous scanning method is used, the rate is 4°/min, the range is 5–90°, Cu target, K_α radiation. In the SEM test, the acceleration voltage is 5 kV, the magnification is 10 k–30 k times, and the scale is 2–20 μm.

4. Result analysis

4.1. Slump and slump-flow

By measuring the slump and slump-flow of backfill slurry with different solid waste content, the results are shown in Fig. 5(a)-(d).

It can be seen from Fig. 5 that the slump-flow and slump of the backfill slurry at the mass concentration of 76% are greater than those of the backfill slurry at the mass concentration of 78%, indicating that the mass concentration has a negative effect on the slump and slump-flow of the backfill slurry.

The four kinds of solid wastes have different effects on the slump and slump-flow of backfill slurry. It can be seen from Fig. 5(a) that when the mass concentration is 76% and 78%, with the increase of G/SW, the slump-flow of the backfill slurry increases slowly, and the variation range is 50–56 cm. The slump of the backfill slurry increases first and then decreases with the increase of G/SW, that is, when G/SW = 9%–23%, the slump of the backfill slurry increases gradually; when G/SW = 23%, the slump is the largest, which are 14.2 cm (76%) and 14 cm (78%), respectively. When G/SW > 23%, the slump of the backfill slurry decreases, and the accumulation phenomenon of gangue gradually becomes more obvious. The reason is that the friction of gangue particles in irregular shapes is large, and when the content of gangue particles increases, the backfill material forms a certain accumulation body, resulting in a small expansion range of the backfill slurry flowing outward [22].

It can be seen from Fig. 5(b) that the slump and slump-flow of the backfill slurry show a slow downward trend with the increase of fly ash content. When the mass concentration is 76% and 78%, the slump of the backfill slurry with FA/SW = 39% is 2.82% and 2.84% lower than that of the slurry with FA/SW = 11%, respectively, with a decrease of 10.18% and 7.59%. It can be seen that the slump and slump-flow of the backfill slurry show a slow downward trend with the increase of the amount of fly ash, especially the influence of fly ash on the slump-flow of the slurry is more obvious. It shows that fly ash has good water absorption, and the increase in its content leads to a decrease in fluidity.

Fig. 5 (c) shows the influence of different gasification coarse slag content on the slump and slump-flow of backfill slurry. With the increase of the content of the gasification coarse slag, the slump and slump-flow of the backfill slurry show an obvious downward trend. When the mass concentration is 76% and 78%, the slump of the backfill slurry with GCS/SW = 42% is 4.90% and 4.97% lower than that of the slurry with GCS/SW = 13%, and the slump-flow is reduced by 8.93% and 11.32%, respectively. It can be seen that the gasification coarse slag has a significant negative impact on the slump-flow of the backfill slurry. In the experiment, it was found that when GCS/SW exceeded 37%, the backfill slurry also showed an obvious accumulation phenomenon. The main reason is that the content of gasification coarse slag is high, and surface of its particle is rough [33], which is not conducive to collapse and flow.

It can be seen from Fig. 5(d) that with the increase of DG/SW from 11% to 39%, the slump-flow of backfill slurry at the mass concentration of 76% and 78% increases from 50 cm to 48 cm–54.7 cm and 52.2 cm, respectively, with an increase of 9.4% and 8.75%; The slump of the backfill slurry increased from 13.9 cm to 13.7 cm–14.2 cm and 14.1 cm, with an increase of 2.11% and 2.92%, respectively, indicating that the influence of desulfurization gypsum on the slump and slump-flow of the backfill slurry shows a positive effect. The reason is that desulfurization gypsum is powdery, and its particles contain crystal water, which has certain lubricity and increases the fluidity of backfill materials [34].

4.2. Bleeding rate

To study the effect of different solid waste content on the bleeding rate of the backfill slurry, the bleeding rate of the backfill slurry in each experimental group was calculated, and the results are shown in Fig. 6(a)-(d).

The four kinds of solid waste showed different effects on the bleeding rate of backfill slurry. With the increase of gangue content, the bleeding rate of backfill slurry increases obviously; When G/SW is increased from 9% to 33%, the bleeding rate of backfill slurry with mass concentration of 76% and 78% is increased from 5.2% to 4.2%–7.5% and 6.4% respectively, indicating that the gangue is difficult to dissolve in water and has poor water absorption. When the FA/SW increased from 11% to 39%, the bleeding rate of the backfill slurry with a mass concentration of 76% and 78% decreased from 6.2% to 5.5%–3.5% and 3.2%, respectively. It can be seen that fly ash can be well integrated with water, and the increase of its content will lead to bleeding rate decrease of backfill slurry [35]. When the content of gasification coarse slag gradually increased, the bleeding rate of the backfill slurry showed a slow increase trend; when GCS/SW < 33%, the bleeding rate of the backfill slurry increased slowly, while GCS/SW increases from 33% to 39%, the bleeding rate of backfill slurry with mass concentration of 76% and 78% increases from 5.2% to 4.2%–6.2% and 5.5%, respectively, with a significant increase. It can be seen that the gasification coarse slag has limited water absorption. The desulfurization gypsum has a negative effect on the bleeding rate of the backfill slurry. When the DG/SW is 11%–27%, the bleeding rate of the backfill slurry increases slowly, and the bleeding rate of the backfill slurry with a mass concentration of 76% and 78% varies from 4.4% to 5.2% and 4%–4.3% respectively. The desulfurization gypsum has a negative effect on the bleeding rate of the backfill slurry. When the DG/SW is 11%–27%, the bleeding rate of the backfill slurry increases slowly, and the bleeding rate of the backfill slurry with a mass concentrations of 76% and 78% varies from 5.2% to 6.8% and 4.2%–5.8% respectively, and the bleeding rate increases significantly. It can be seen that when DG/SW is greater than 27%, the desulfurization gypsum particles contain crystal water and are saturated with water, resulting in a significant increase in the bleeding rate of backfill slurry.

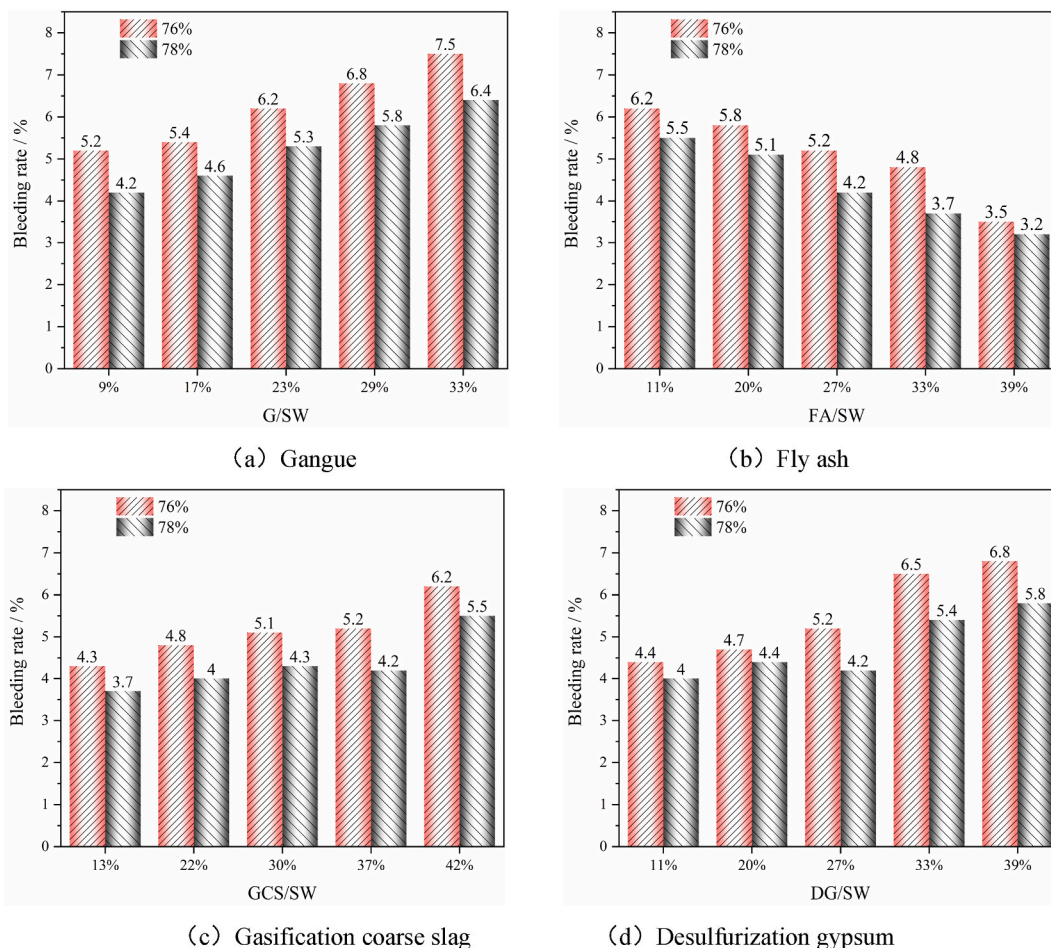


Fig. 6. Test results of backfill material bleeding rate.

4.3. Early strength

The maximum load of the specimens cured for 3 days and 7 days during failure was tested by uniaxial compression, and the results are shown in Fig. 7(a) ~ (d).

It can be seen from Fig. 7 (a)–(d) that due to the small cement content, the maximum bearing load of the specimen during compression failure is generally small, with the variation range of 0.55–1.15 kN and the corresponding compressive strength variation range of 0.11–0.23 MPa. The 7-day strength of the specimen was significantly higher than its 3-day strength, indicating that the curing time was positively correlated with the compressive strength of the specimen in a short time. In the same curing time, the mass concentration of the backfill material is generally positively correlated with its early strength, that is, the early strength of the specimen with a mass concentration of 78% is generally greater than that of the specimen with the mass concentration of 76%, but the difference in strength is small.

Four kinds of solid waste materials have different effects on the early strength of the specimens. With the increase of gangue content, the early strength of the specimen showed a trend of increasing first and then decreasing (Fig. 7(a)), that is, when the G/SW was 9–23%, the early strength of the specimen increased slowly, while When G/SW is 23–33%, the early strength of the specimen decreases slowly; It shows that the gangue shows obvious aggregate supporting effect when its content is small. With the increase of the gangue content, the cementitious material becomes less and the supporting effect of the gangue decreases [22]. In this experiment, the specimen with G/SW of 23% had the highest strength at 3 days and 7 days, and the maximum strength was 0.15 MPa and 0.22 MPa (mass concentration 78%), respectively. It can be seen from Fig. 7 (b) that the content of fly ash has a positive effect on the early strength of the specimen. With the increase of FA/SW from 11% to 29%, the 3-day and 7-day strength of the specimens with 78% mass concentration increased from 0.12 MPa to 0.16 MPa–0.16 MPa and 0.22 MPa, respectively, with an increase of 33.33% and 37.50%. Fig. 7(c) shows that when GCS/SW increases from 13% to 37%, the strength of the specimen with a mass concentration of 78% increases from 0.12 MPa to 0.15 MPa–0.14 MPa and 0.19 MPa at 3 days and 7 days, respectively, and the early strength shows a slow increasing trend. While GCS/SW increased from 37% to 42%, the early strength of the specimen increased slightly, or even remained basically unchanged, indicating that when the GCS/SW was not greater than 37%, the gasification coarse slag had a significant positive impact on the early strength of the specimen, and its particles form a backfill and supporting role in the aggregate. When GCS/SW is greater than 37%, the influence of gasification coarse slag on the backfilling and supporting of aggregate becomes smaller. It can be

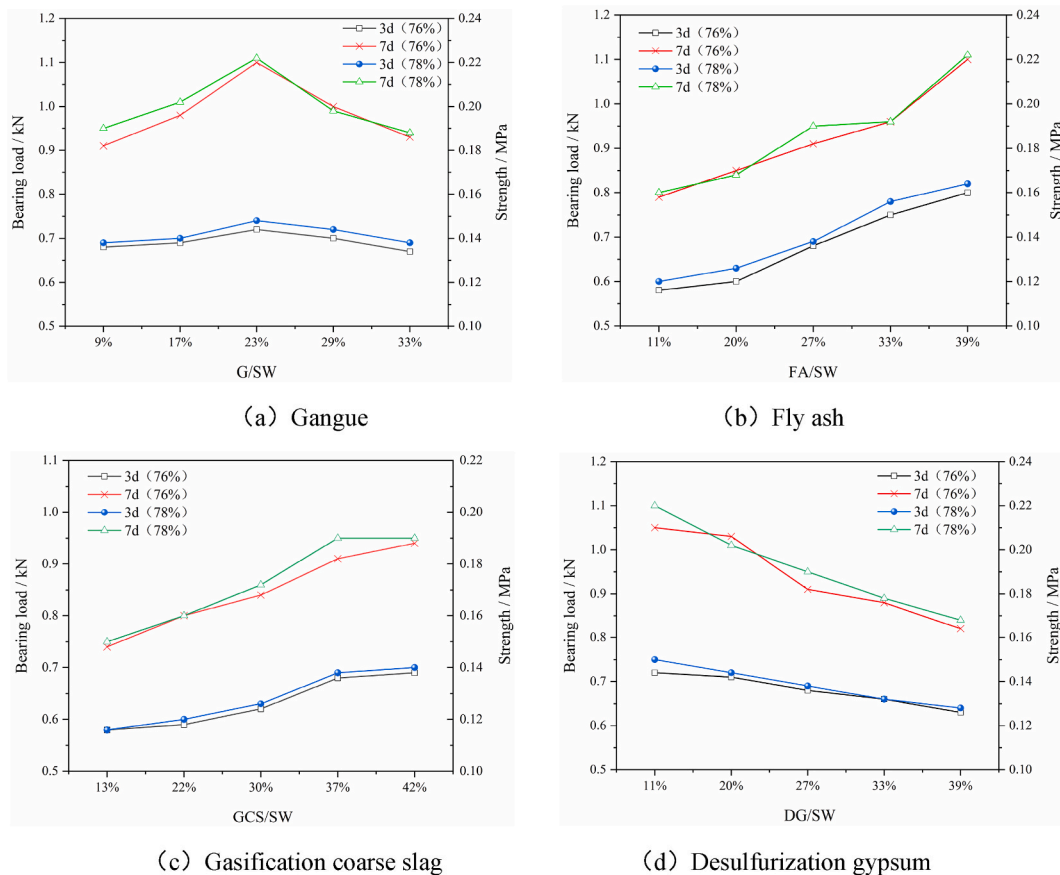


Fig. 7. Effect of different solid wastes on early strength of backfill materials.

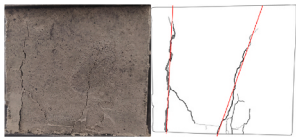
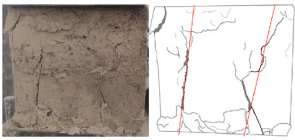
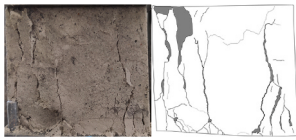
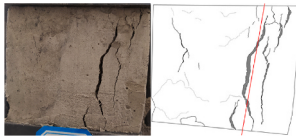
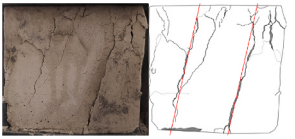
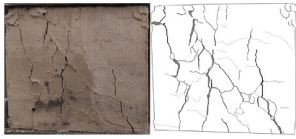
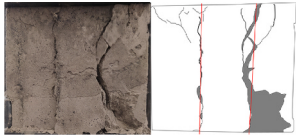
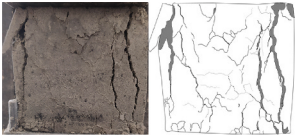
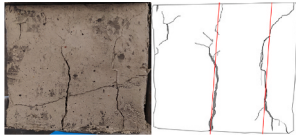
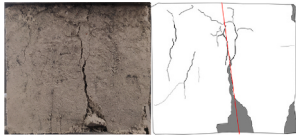
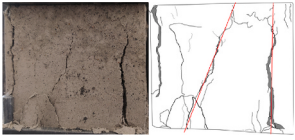
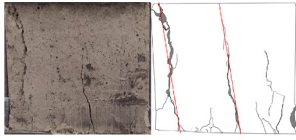
seen from Fig. 7 (d) that with the increase of desulfurized gypsum content, the strength of the specimen at 3 days and 7 days showed a slow decreasing trend. When DG/SW increased from 11% to 39%, the 3-day and 7-day strength of the specimen decreased from 0.15 MPa to 0.22 MPa–0.13 MPa and 0.17 MPa, respectively, with a decrease of 13.33% and 20.91%. It can be seen that the cementation performance of desulfurization gypsum in this experiment is poor.

4.4. Failure characteristics

To study the failure characteristics of backfill specimens after the stress peak, the specimens with the relative proportion of each variable factor of 2 and 4 and the curing time of 3 days and 7 days were selected as the research objects, as shown in Table 4.

It can be seen from Table 4 that no matter whether the content of various solid wastes in the backfill materials is high (relative proportion is 4) or low (relative proportion is 2), or the curing time of the specimens is 3 days or 7 days, the specimens composed of four kinds of solid wastes generally undergo longitudinal compression, transverse expansion and deformation during the compression process, and the concave surfaces formed by block spalling appear in the upper and lower areas of some specimens. According to the factors such as the width, quantity, distribution and influence of the cracks in the specimen surface, the typical failure modes are divided into three modes, i.e. crack intensive failure, single main crack penetration splitting failure and double main crack conjugate splitting failure. The crack-intensive failure mode shows that there is no obvious main crack with a large width that penetrates upper and lower parts in the middle area of the specimen surface, but many dense and small narrow cracks, the width of which is generally not more than 0.5 mm. The narrow cracks on both sides of individual specimens expand laterally and longitudinally under continuous compression, such as the specimen with a relative proportion of gasification coarse slag of 4 and a curing time of 3 days. The single main crack penetration splitting failure mode shows that there is a main crack that penetrates the upper and lower parts on the surface of the specimen. The maximum crack width exceeds 1 mm, which plays a major role in the splitting failure of the specimen. A number of short cracks with a width less than 0.5 mm are developed nearby. This failure mode exists in the specimens with the relative proportion of desulfurization gypsum or fly ash of 2 and the curing time of 3 days. The double main crack conjugate splitting failure mode is mainly characterized by the large and small two main cracks on the specimen surface, which jointly form a penetrating splitting failure on the specimen. The width of main cracks is generally between 0.5 and 1 mm, that of individual main cracks exceeds 1 mm, and a number of short cracks with a width less than 0.5 mm are generated nearby. This failure mode appears most in the experiment, for example, the specimen with the relative proportion of gasification coarse slag of 2 and the curing time of 3 days.

Table 4
Failure mode of backfill specimen.

Variable	The relative proportion of variables is 2 Curing time is 3-day	The relative proportion of variables is 4 , Curing time is 3-day	The relative proportion of variables is 4 Curing time is 7-day
Gangue	 double main crack conjugate splitting failure	 double main crack conjugate splitting failure	 Crack-intensive failure
Fly ash	 Single main crack penetration splitting failure	 double main crack conjugate splitting failure	 Crack-intensive failure
Gasification coarse slag	 double main crack conjugate splitting failure	 Crack-intensive failure	 double main crack conjugate splitting failure
Desulfurization gypsum	 Single main crack penetration splitting failure	 double main crack conjugate splitting failure	 double main crack conjugate splitting failure

4.5. Thermal stability

To fully understand the influence of the four solid wastes on the performance of the specimen, the thermal stability was analyzed by the (Thermal Gravity) TG, (Derivative Thermogravimetry) DTG and (Differential Thermal Analysis) DTA curves obtained by the TGA test. The results are shown in Fig. 8(a)–(d).

It can be found from Fig. 8(a)–(d) that the variation trends of TG, DTG and DTA curves with different proportions of various solid wastes are basically the same. When the temperature is about 55–65 °C and 110–120 °C, TG curves with different proportions of various solid wastes show an obvious sudden drop, DTG curves and DTA curves generally show obvious characteristic peaks, which shows that when the temperature is about 55–65 °C and 110–130 °C, the backfill material generally occurs the vaporization of liquid water and crystal water and the dehydration of hydration products. The water loss reaction rate between this temperature range is the largest and absorbs heat. When the temperature is higher than 130 °C, the TG curve of the specimen decreases slowly, the DTG curve changes gently, and the DTA curve shows a curved arc, indicating that with the continuous increase of temperature, the backfill material undergoes a slow decomposition reaction, and the reaction rate becomes small, and the whole process is exothermic.

There are differences in the thermal stability of the specimens with different contents of solid waste. Fig. 7(a) shows that the variation range of the TG curve with G/SW = 33% is smaller than that of the TG curve with G/SW = 17%, and the peaks of the DTG and DTA curves are both lower in the range of 115 ± 1 °C, indicating that when the content of gangue is large, the weight loss of the material is less as the temperature increases due to the lower water content in gangue particles. Fig. 8(b) and (c) show that the changing trends of TG, DTG and DTA curves with different contents of fly ash and gasification coarse slag are basically consistent with those in Fig. 8(a), indicating that the content of fly ash and gasification coarse slag increases, and the thermal stability of the specimen is better. The reason is that both fly ash and gasification coarse slag are products of coal combustion at high temperature and are inert to high temperature (≤ 800 °C) [36,37]. The changing trend of TG, DTG and DTA curves in Fig. 8(d) is different from that in Fig. 8(a)–(c). When DG/SW = 39%, at 110–122 °C, the TG curve has a larger decrease, the peak value of the DTG curve is higher, and the value of the DTA curve is larger, indicating that the content of desulfurization gypsum is larger, and the dehydration and thermal decomposition reactions of the specimen are more significant, which is mainly because there is crystal water in desulfurization gypsum.

4.6. XRD analysis

The composition of the specimen with the solid waste ratio of FA:GCS:DG:G = 3:4:3:1 is analyzed by XRD before and after the TGA

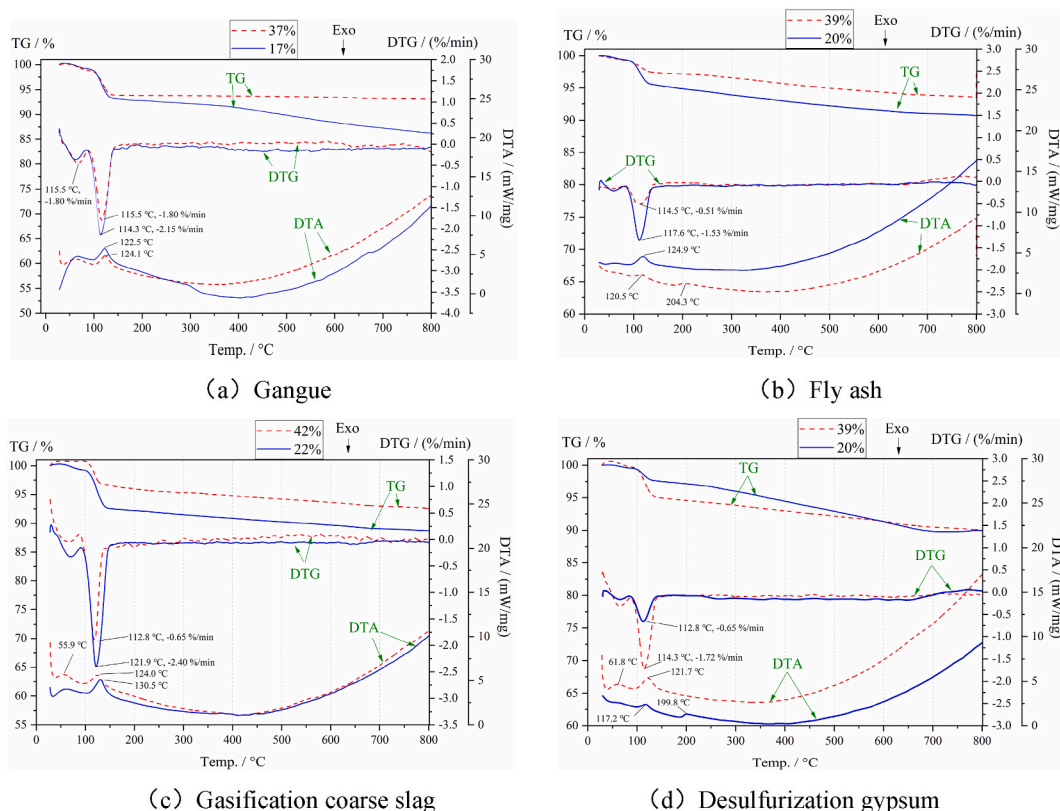
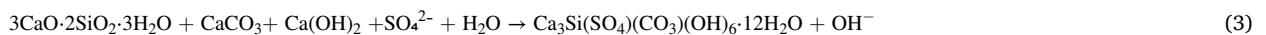
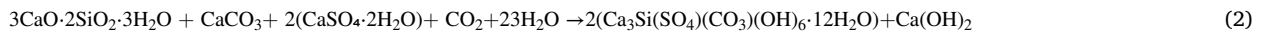


Fig. 8. TGA results of backfill specimens.

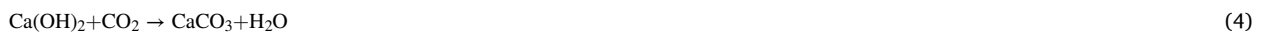
test, and the composition change of the backfill material was deeply analyzed. The results are shown in Fig. 9.

It can be seen from Fig. 9 that the characteristic peaks pulses of gypsum are the most and the intensity is highest before TGA, indicating that the content of gypsum in solid waste paste backfill is the most, followed by quartz.

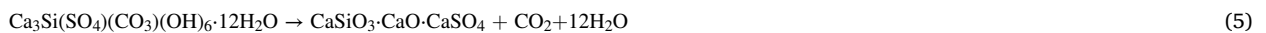
It can be seen from Figs. 4 and 9 that most of the gypsum and quartz with low activity in the coal-based solid waste backfill material do not participate in the hydration reaction. In addition, there is a weak characteristic peak of thaumasite in the XRD pattern, and its chemical formula is $\text{Ca}_3\text{Si}(\text{SO}_4)(\text{CO}_3)(\text{OH})_6 \cdot 12\text{H}_2\text{O}$. The content of this product is small, but it can cause the strength loss of the solid waste backfill material [38], which is one of the main factors for the generally low strength of the specimens in this experiment. In this experiment, the production mechanism of thaumasite is that tricalcium silicate (C_3S) in cement reacts with water to form C–S–H gel and CH ($\text{Ca}(\text{OH})_2$), and SiO_3^{2-} released from C–S–H gel reacts with CO_3^{2-} and SO_4^{2-} released from solid waste to form thaumasite under alkaline water environment and appropriate temperature. SO_4^{2-} may be provided by desulfurization gypsum, so the increase in the content of desulfurization gypsum will promote the formation of thaumasite in the backfill material, resulting in a decrease in the strength of the backfill. The chemical reaction formula is as Eqs. (1)–(3) [39].



The $\text{Ca}(\text{OH})_2$ produced by the reaction does not exist as the final product, and it reacts with CO_2 dissolved in water to generate CaCO_3 , which becomes one of the carbonate sources in the formation process of thaumasite. The chemical reaction formula is as Eq. (4).



After the TGA test, the phase of solid waste backfill material changed. The characteristic peak of anhydrite appears in the XRD pattern, and the characteristic peak intensity and quantity of anhydrite decrease obviously compared with that of gypsum, indicating that gypsum has undergone an obvious dehydration reaction after the TGA test to generate anhydrite. The characteristic peak intensity and quantity of quartz are basically unchanged, indicating that quartz has good stability at high temperatures. The characteristic peak of thaumasite almost disappears after the TGA test, which indicates that thaumasite undergoes dehydration and decomposition reaction at high temperatures to generate amorphous products. The decomposition reaction formula is as Eq. (5):



4.7. SEM analysis

The micromorphology of the specimen with the solid waste ratio of FA: GCS: DG: G = 3:4:3:1 is analyzed by SEM before and after the TGA test, as shown in Fig. 10.

It can be seen from Fig. 10(a) that at room temperature, there are many fine impurities in the backfill material, each solid waste

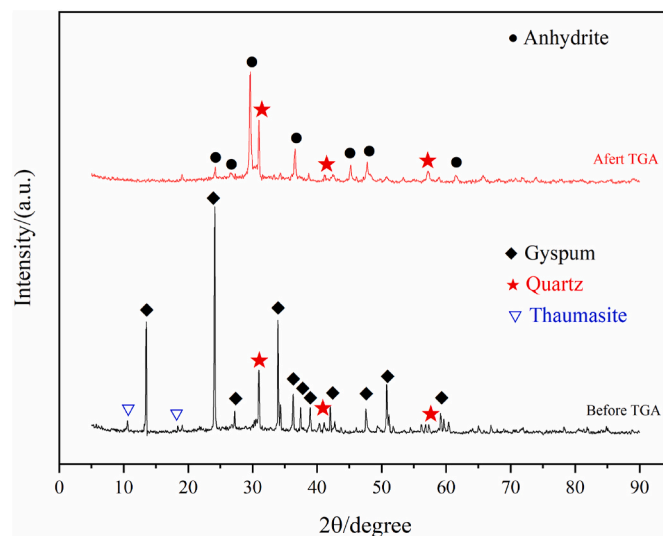


Fig. 9. XRD results before and after TGA.

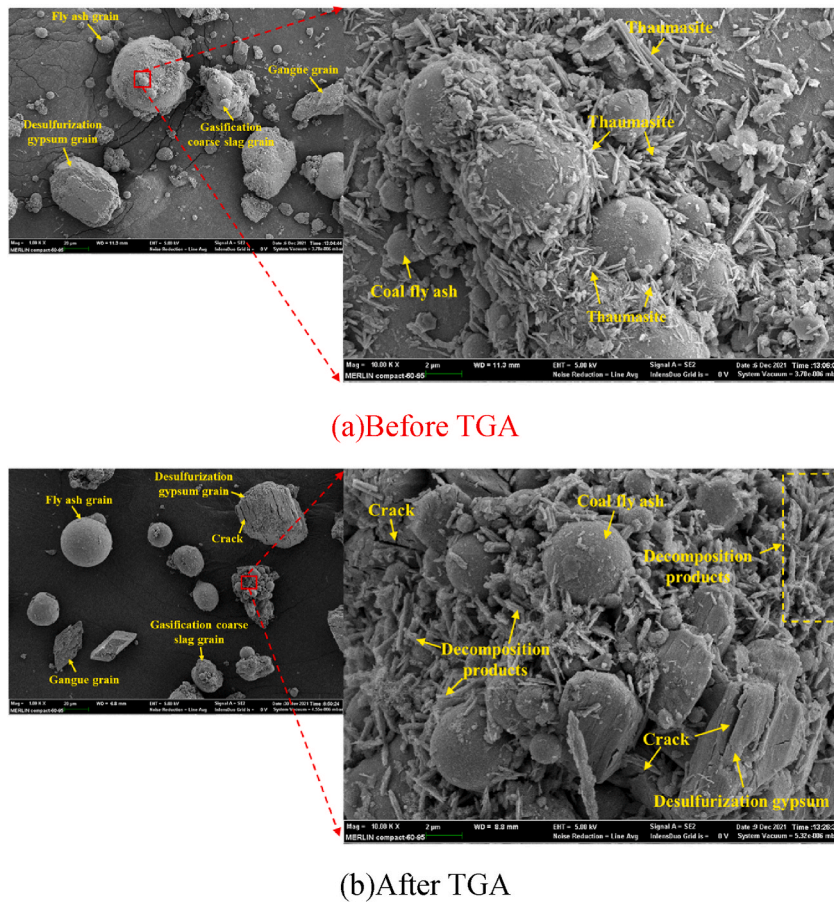


Fig. 10. SEM results before and after TGA.

particle is independent and has different shapes. The gangue granules are irregular blocks, and the fly ash granules are spheres with smooth surfaces; The gasification coarse slag granules are irregular in shape, the surface is uneven, and there are a few pits; The desulfurization gypsum granules are relatively regular blocks with small pores on the surface, showing an uneven shape. There is an intrinsic relationship between the microstructure of each solid waste particle and the fluidity of the backfill slurry. For example, due to the irregular block shape of gangue particles and the irregular particle shape of gasification coarse slag, the increase of them is not conducive to the slurry flow. The increase of fly ash content is beneficial to reduce the slurry conveying resistance due to the smooth spherical structure of the fly ash particle surface, the effect of the microstructure of desulfurization gypsum is also the same. Through the local enlargement of the mixture particles, it is found that in addition to some spherical fly ash particles that are not involved in the reaction, there are a large number of fine needle rods and hexagonal prism products on the surface of the mixture particles. According to the analysis of Fig. 9 and the literature [39], it can be seen that this product is thaumasite particles.

After TGA with a temperature up to 800 °C, the fine impurities between the solid wastes are significantly reduced, as shown in Fig. 10(b). The granule surface of fly ash and gasification coarse slag has no obvious change, while the surface of gangue granules has delamination and many cracks, and the compactness is greatly reduced. The desulfurization gypsum granules also have obvious changes after high temperature, with dense longitudinal cracks on the surface, and the surface is uneven, just like burned wood. Through local amplification, it is found that microcracks are locally generated on the surface of the mixture particles, the volume of the thaumasite particles is reduced, and there are folds on the surface of the particles, and the edges are flocculent. Also, there are obvious burning marks on the surface of backfill material particles.

5. Conclusions

With the increase of fly ash content, the fluidity of the backfill slurry decreases, but the early strength increases; When G/SW < 23%, the increase of gangue content is beneficial to improve the fluidity and early strength of the backfill slurry; The gasification coarse slag has a negative effect on the fluidity of backfill slurry, and it is beneficial to improve the early strength when GCS/SW < 37%; Properly increasing the content of desulfurized gypsum can improve the fluidity of backfill slurry, but it is unfavorable to the early strength. The typical failure modes of the specimens are mainly divided into crack-intensive failure, single main crack penetration

splitting failure and double main crack conjugate splitting failure.

The changing trend of TG, DTG and DTA curves of solid waste backfill materials is consistent, and the endothermic dehydration reaction of adsorption water and crystal water occurs at 55–65 °C and 110–130 °C. With the increase of temperature, the specimen undergoes continuous and slow decomposition exothermic reaction. Increasing the content of gangue, fly ash and gasification coarse slag and reducing the content of desulfurized gypsum can make the specimen lose less weight and have better thermal stability. At room temperature, the minerals in the solid waste samples are mainly gypsum and quartz, as well as a small amount of needle rod-shaped and hexagonal prismatic thaumasite. After TGA test, anhydrite is formed by dehydration of gypsum, and longitudinal cracks are distributed on the particle surface; quartz does not react at high temperatures, and thaumasite undergoes dehydration and decomposition reaction at high temperatures, resulting in volume reduction and edge flocculation.

Author contribution statement

Xinyuan Zhao: Conceived and designed the experiments; Performed the experiments; Analyzed and interpreted the data; Wrote the paper.

Ke Yang, Zhen Wei, Xiang He: Conceived and designed the experiments; Contributed reagents, materials, analysis tools or data.

Ruiyi Chen: Performed the experiments.

Data availability statement

Data will be made available on request.

Additional information

No additional information is available for this paper.

Declaration of competing interest

The authors declare no conflict of interest.

Acknowledgements

This paper was supported by National Key R&D Program of China (2019YFC1904304), Institute of Energy, Hefei Comprehensive National Science Center (21KZS217), University Synergy Innovation Program of Anhui Province (GXXT-2021-017) and 2022 Anhui New Era Education Quality Engineering Project (Graduate Education) (2022cxcsj110).

References

- [1] Y. Tang, X. Guo, Q. Xie, R.B. Finkelman, S. Han, B. Huan, X. Pan, Petrological characteristics and trace element partitioning of gasification residues from slagging entrained-flow gasifiers in Ningdong, China, *Energy & Fuels* 32 (3) (2018) 3052–3067.
- [2] N. Jiang, J.H. Zhao, X.Z. Sun, L.Y. Bai, C.X. Wang, Use of fly-ash slurry in backfill grouting in coal mines, *Heliyon* 3 (11) (2017).
- [3] F.W. Zhang, Y.Y. Li, J.H. Zhang, X. Gui, X.H. Zhu, C.M. Zhao, Effects of slag-based cementitious material on the mechanical behavior and heavy metal immobilization of mine tailings based cemented paste backfill, *Heliyon* 8 (9) (2022).
- [4] Y. Wang, Y.X. Lei, S.Y. Wang, Green mining efficiency and improvement countermeasures for China's coal mining Industry, *Front. Energy Res.* 8 (2020).
- [5] Q.S. Chen, Q.L. Zhang, C.C. Qi, A. Fourie, C.C. Xiao, Recycling phosphogypsum and construction demolition waste for cemented paste backfill and its environmental impact, *J. Clean. Prod.* 186 (2018) 418–429.
- [6] X. Zhao, K. Yang, X. He, Z. Wei, X. Yu, J. Zhang, Study on mix proportion optimization and microstructure of coal-based solid waste (CSW) backfill material based on multi-objective decision-making model, *Materials* 15 (23) (2022).
- [7] S.H. Yin, A.X. Wu, K.J. Hu, Y. Wang, Y.K. Zhang, The effect of solid components on the rheological and mechanical properties of cemented paste backfill, *Miner. Eng.* 35 (2012) 61–66.
- [8] X.G. Zhang, J.W. Bai, H. Wang, N. Jiang, Study on proportioning test of coal solid waste paste filling material, *Adv. Mater. Res.* 524–527 (2012) 1086–1091.
- [9] X. Zhao, K. Yang, X. He, Z. Wei, J. Zhang, X. Yu, Study on characteristics of compression deformation and post-peak stress rebound for solid waste cemented body, *Minerals* 13 (1) (2023) 108.
- [10] H.F. Qiu, C. Liang, B.B. Tu, L. Liu, F.S. Zhang, W.Y. Lv, Study on mechanical properties of cemented backfill with different mineral admixtures, *Construct. Build. Mater.* 367 (2023).
- [11] M. Fall, M. Benzaouza, E.G. Saa, Mix proportioning of underground cemented tailings backfill, *Tunn. Undergr. Space Technol.* 23 (1) (2008) 80–90.
- [12] J.Q. Zhang, K. Yang, X. He, Z. Wei, X.Y. Zhao, J.J. Fang, Experimental study on strength development and engineering performance of coal-based solid waste paste filling, *Material, Metals* 12 (7) (2022).
- [13] H.B. Wei, B.L. Xiao, Q. Gao, Flow properties analysis and identification of a fly ash-waste rock mixed backfilling slurry, *Minerals* 11 (6) (2021) 12.
- [14] D. Chen, T. Cao, R. Chen, C. Li, Optimization analysis of mechanical properties of fly ash-based multicontent gasification slag paste filling material, *Adv. Civ. Eng.* 2022 (2022), 5908317.
- [15] B. Koohestani, A. Koubaa, T. Belem, B. Bussiere, H. Bouzazhah, Experimental investigation of mechanical and microstructural properties of cemented paste backfill containing maple-wood filler, *Construct. Build. Mater.* 121 (2016) 222–228.
- [16] Y.S. Tang, L.F. Zhang, H.Y. Lü, Study on proportion optimization of coal - based solid wastes filling materials, *J. Mining Sci. Technol.* 4 (4) (2019) 327–336.
- [17] I. Cavusoglu, E. Yilmaz, A.O. Yilmaz, Sodium silicate effect on setting properties, strength behavior and microstructure of cemented coal fly ash backfill, *Powder Technol.* 384 (2021) 17–28.
- [18] B. Zhao, H. Wang, D. Zhai, Y. Ma, Q. Wei, J. Wang, Performance of a new type of backfilling material based on loess-fly ash, *Bull. Chin. Ceram. Soc.* 41 (1) (2022) 199–208.
- [19] H.Q. Jiang, M. Fall, Y.H. Li, J. Han, An experimental study on compressive behaviour of cemented rockfill, *Construct. Build. Mater.* 213 (2019) 10–19.

- [20] Y. Xu, L. Zhang, Y. Lu, Influences of fly ash slag and silica fume on cement mortar fluidity and early strength, *Concrete* (9) (2005) 39–41.
- [21] G.N. Sun, Y. Huang, Effect of fly ash on properties of mixed aggregate plastering mortar, *Integr. Ferroelectr. Int. J.* 219 (1) (2021) 134–144.
- [22] S. Wang, Y. Li, Q. Li, Z. Wang, Y. Wang, Influence of gangue gradation coefficient on the performance of filling material based on talbol theory, *J. Mining Saf. Eng.* 4 (9) (2022) 683–692.
- [23] S.J. Yang, X. Xing, S. Su, F.L. Wang, Experimental study on rheological properties and strength variation of high concentration cemented unclassified tailings backfill, *Adv. Mater. Sci. Eng.* (2020) 2020.
- [24] X. Deng, J. Zhang, B. Klein, N. Zhou, B. deWit, Experimental characterization of the influence of solid components on the rheological and mechanical properties of cemented paste backfill, *Int. J. Miner. Process.* 168 (2017) 116–125.
- [25] B. Ercikdi, T. Yilmaz, G. Külekci, Strength and ultrasonic properties of cemented paste backfill, *Ultrasonics* 54 (1) (2014) 195–204.
- [26] M.L. Walske, H. McWilliam, J. Doherty, A. Fourie, Influence of curing temperature and stress conditions on mechanical properties of cementing paste backfill, *Can. Geotech. J.* 53 (1) (2015) 148–161.
- [27] X. Zhao, K. Yang, X. He, Z. Wei, J. Zhang, Study on proportioning experiment and performance of solid waste for underground backfilling, *Mater. Today Commun.* 32 (2022), 103863.
- [28] H.F. Qiu, F.S. Zhang, L. Liu, C. Huan, D.Z. Hou, W. Kang, Experimental study on acoustic emission characteristics of cemented rock-tailings backfill, *Construct. Build. Mater.* 315 (2022).
- [29] D. Deng, Y. Gao, S. Wu, Liquidity detection based on the slump testing of coarse aggregate filling material, *J. Beijing Univ. Civil Eng. Arch.* 25 (1) (2009) 30–33.
- [30] X.J. Lü, Z.J. Jin, S.G. Hu, L. Zhang, Study on rheological property and filling capacity of the filling slurry with fine tailings, *Metal. Mine* (5) (2011) 32–35.
- [31] J.P. Qiu, Z.B. Guo, L. Yang, H.Q. Jiang, Y.L. Zhao, Effect of tailings fineness on flow, strength, ultrasonic and microstructure characteristics of cemented paste backfill, *Construct. Build. Mater.* 263 (2020).
- [32] A.W. Saak, H.M. Jennings, S.P. Shah, A generalized approach for the determination of yield stress by slump and slump flow, *Cement Concr. Res.* 34 (3) (2004) 363–371.
- [33] R. Zhang, X. Li, K. Zhang, P. Wang, P. Xue, H. Zhang, Research on the application of coal gasification slag in soil improvement, *Processes* 10 (12) (2022) 2690.
- [34] J. Lu, B. Zhao, X. Chen, J. Cao, Preparation of the high-quality gypsum by dihydrate FGD, *J. Synth. Cryst.* 1 (45) (2016).
- [35] L. Bian, Experimental study on cement paste fluidity of self-compacting concrete, *Shanxi Arch.* 41 (19) (2015) 103–104.
- [36] X.D. Liu, Z.W. Jin, Y.H. Jing, P.P. Fan, Z.L. Qi, W.R. Bao, J.C. Wang, X.H. Yan, P. Lv, L.P. Dong, Review of the characteristics and graded utilisation of coal gasification slag, *Chin. J. Chem. Eng.* 35 (2021) 92–106.
- [37] G. Xu, X.M. Shi, Characteristics and applications of fly ash as a sustainable construction material: a state-of-the-art review, *Resour. Conserv. Recycl.* 136 (2018) 95–109.
- [38] Y.M. Song, S.L. Zhou, Z.J. Wang, B. Wang, J.S. Qian, Mechanism of thaumasite formation in concrete, *J. Wuhan Univ. Technol.-Mater. Sci. Ed.* 32 (4) (2017) 893–897.
- [39] L. Gao, X. Du, L. Kong, Quantitative analysis on formation mechanism of thaumasite, *J. Chin. Ceram. Soc.* 40 (5) (2012) 711–714.